16th World Conference on Earthquake, 16WCEE 2017
Santiago Chile, January 9th to 13th 2017
Paper N° 375
Registration Code: S-U1463152774

The verification of the pseudo point-source model through simulations of past earthquakes in Japan

K. Nakano[(1)], S. Sakai[(2)]

[(1)] Researcher, Technical Research Institute, HAZAMA ANDO CORPORATION, nakano.kenichi@ad-hzm.co.jp
[(2)] Manager, Technical Research Institute, HAZAMA ANDO CORPORATION, sakai.shigeki@ad-hzm.co.jp

Abstract

This study aims to confirm the validity of the pseudo point-source model by introducing the results of strong ground motion simulations of four earthquakes in Japan based on this model. Herein, “the validity” means that the simulation results of this model do not significantly fluctuate according to different researchers. We introduce the potential of the pseudo-point source model by simulating three crustal earthquakes (i.e., the mid Niigata prefecture earthquake in 2004, the central Chiba prefecture earthquake in 2005, and the northern Nagano prefecture earthquake in 2014) and a plate-boundary earthquake (the Tokachi-oki earthquake in 2003) in Japan, using the empirical site amplification. Our calculation results show a good agreement with the waveforms and the Fourier spectra of observations at each earthquake. Therefore, the validity of this model was verified by this study. However, we did not estimate the parameters (e.g., radiation pattern) before the calculations; we used the site amplifications estimated by Nakano et al., which are different from those by Nozu or Hata and Nozu.

Keywords: The pseudo point-source model, strong ground motions, empirical site amplifications

1. Introduction

Prediction of strong ground motions (e.g., Hartzell [1] and Irikura [2]) is mainly conducted to prevent disasters caused by earthquakes or structural design of architectures. In the former, we must consider the possibility of occurrence of earthquakes, which is larger than our supposition, to predict strong ground motions because of the objective of preventing disasters and protecting human life and properties (for example, by cabinet office in Japan). In the latter, we cannot decide on the strength of the ground motions (e.g., pSv or PGA) as regards the building structural design because of the above-mentioned reasons. In short, the structural design of architectures is based on engineering judgments, which are decided based on the needs of owners. Although judging the strength of ground motions is an extremely critical factor for the building structural design, sufficient time and capital is often not available for the structural design works of buildings and the investigation of the strength or variation of (strong) ground motions because we must adhere to conditions of the contracts and comply with requests by owners. Therefore, we pursue the method, which can calculate the appropriate seismic waves at any target sites, quickly and easily.

In Japan, you need to confirm the structural safety of a high-rise (higher than 60 m) or an isolated building when designing by calculating the responses of buildings to seismic waves in the time domain (i.e., dynamic analysis of structures). Structural designers confirm the structural safety of buildings to ground motions as soon as possible in a limited time. Therefore, we need to quickly evaluate the seismic waves at the target site by using the proper methods for buildings and earthquakes. For example, the empirical Green's function method (EGFM) proposed by Irikura [3, 4] is a common method of estimating seismic waves. Kamae and Irikura [5] or Kamae and Kawabe [6] have confirmed the validity of the EGFM by simulating the 1995 Kobe earthquake and the 2003 Tokachi-oki earthquake in Japan. The integrated wavelength method proposed by Hisada [7] is a synthesis approach effective in calculating strong ground motions at sites composed of a layered half-space.

The simulation methods based on the pseudo-point source model (PPSM, herein) have been proposed by Nozu [8]. He introduced the potential of this method by simulating the strong ground motions of the 2011 off the Pacific coast of Tohoku earthquake. According to the study, the PPSM can explain the velocity waveforms (0.2–2 Hz) and Fourier spectra (0.1–10 Hz) better than any other simulation methods, except for the SPGA model proposed by Nozu [8]. Hata and Nozu [9] reported the reproducibility of the PPSM to crustal earthquakes in Japan.

The waveforms generally consist of amplitudes and phases. The amplitudes are calculated by the product of the source spectra, propagation properties, and site amplification in frequency domains. The imaginary parts of the Fourier spectra of waveforms on the PPSM observed in earthquakes, which have the same relations as that of the source-observation locations you might be interested in, are used for the phase. According to previous papers, the PPSM in the real part is based on the source spectral model proposed by Boore [10] and the site amplification estimated by researchers. The propagation terms are normally assumed to be geometric attenuation and internal damping depending on frequency. The results of the simulations change if you change the above-mentioned parameters.

However, no other study except that of Dr. Nozu and his colleagues in Japan calculates the strong ground motions based on the PPSM. This scarcity in relevant study suggests the necessity of verifying and validating this method. Almost all studies, which reproduce the observation records of earthquakes, have performed the pre-calculation to estimate the optimal parameters of the source model or other characteristics for simulations. Unfortunately, we cannot correctly estimate the strong ground motion characteristics to predict future earthquakes although it is important to know it by simulating past earthquakes. We investigate the potential of the PPSM by simulating three crustal earthquakes (i.e., the mid Niigata prefecture earthquake in 2004, the central Chiba prefecture earthquake in 2005, and the northern Nagano prefecture earthquake in 2014) and a plate-boundary earthquake (i.e., the Tokachi-oki Earthquake in 2003) in Japan using the site amplifications estimated by Nakano et al. [11].

This study aims to confirm the validity of the PPSM by introducing the results of strong ground motion simulations of four earthquakes in Japan based on this model. Here, "the validity" means that the simulation results of this model do not significantly fluctuate according to different researchers.

2. Calculation method based on the PPSM

The prediction of strong ground motions based on the PPSM is calculated by Eq. (1) as follows:

$$F^{PRE}(f) = |S(f)| \times |P(f)| \times |G(f)| \times O(f) / |O(f)|_P \tag{1}$$

where $F^{PRE}(f)$ is the acceleration Fourier amplitudes at the surface; $S(f)$ is the source spectrum; $G(f)$ is the site amplification from the bedrock to the surface; and $O(f)$ is the Fourier spectrum calculated from the observed seismic waves with a propagation pass similar to the target earthquake. $P(f)$ is modeled by Eq. (2), which shows the attenuation effects consisting of geometrical attenuations and internal damping (or scattering damping) in the crust. We assume that the geometrical attenuation follows 1/R (where R is the propagation distance). Suffix "P" means we perform the Parzen window (0.05 Hz) to $O(f)$ in the frequency domain. | | shows the absolute value of $O(f)$.

$$|P(f)| = \frac{1}{R} \cdot \exp\left(-\frac{\pi \cdot f \cdot R}{V_S \cdot Q(f)} \right) \tag{2}$$

where R is the hypocentral distance; V_S is the S-wave velocity; and $Q(f)$ is the quality factor depending on the frequency. $S(f)$ is modeled by Boore [10] in Eq. (3) (excluding the term related to f_{max}). We assume the acceleration Fourier spectra in this equation to be

$$|S(f)| = R_{\theta\phi} \cdot FS \cdot P_{RTITN} \cdot \frac{M_0}{4 \cdot \pi \cdot \rho \cdot {V_S}^3} \cdot \frac{(2 \cdot \pi \cdot f)^2}{1 + (f / f_C)^2} \tag{3}$$

where $R_{\theta\varphi}$ is the radiation coefficient, FS is the amplification factor caused by the free surface, P_{RTITN} is the reduction factor that accounts for the partitioning of energy into two horizontal components, and ρ is the density of the source region. $R_{\theta\varphi}$ is assumed to be 0.63 (the average value followed by Boore and Boatwright [14]) in this study. M_0 is the seismic-moment and f_c is the corner frequency. Fig. 1 shows the PPSM based on Eq. (1).

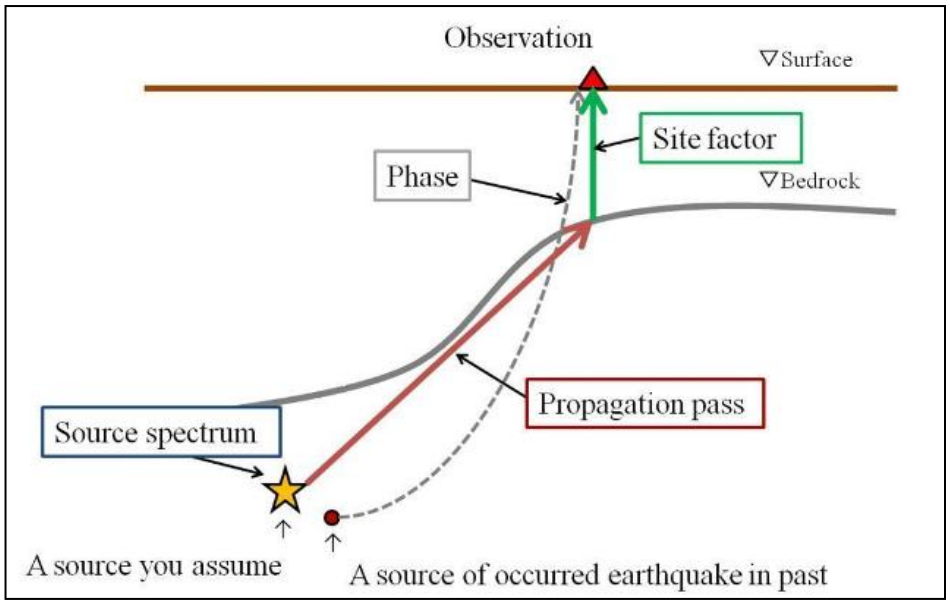

Fig. 1 – Illustration of composition of seismic waves by the pseudo point-source model

3. Application to crustal earthquakes in Japan

3.1 The northwestern Chiba prefecture earthquake in 2005

We participated in the benchmark test [13] proposed by Prof. Hisada at Kogakuin University in Japan to verify and validate the simulation methods for strong ground motions. We confirmed that PPSM, which was one of the stochastic green's function methods, was in a good agreement with the observation records in the simulation of the northwestern Chiba prefecture earthquake in 2005 in the previous paper [14]. We introduced a part of it in this study. Table 1 shows the simulation parameters by the PPSM for the northwestern Chiba prefecture earthquake in 2005. Fig. 2 shows the target and source points. Accordingly, the triangles (▲) and the star symbol (★) represent the calculation and source points, respectively, on the Kanto region in Japan.

Table 1 – Parameters for simulations

Seismic moment M_0 (N・m)	$9.11*10^{17}$
Corner frequency (Hz)	0.75
Radiation coeficient	0.63
FS	2
PRTITN	$1/\sqrt{2}$
Dentisy of seismic bedrock (g/m^3)	3.2
Vs(m/s)	4460
Site amplification	Nakano et al. [11]
Phase characteristics	Observation records (19th May, 2002; M_{JMA}4.6)

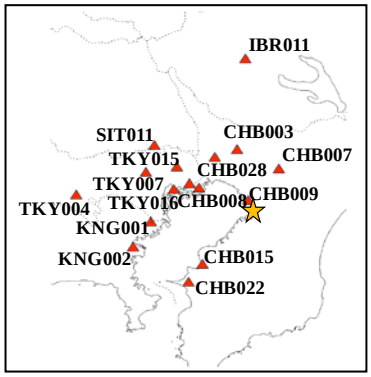

Fig. 2 – Epicenter and observations

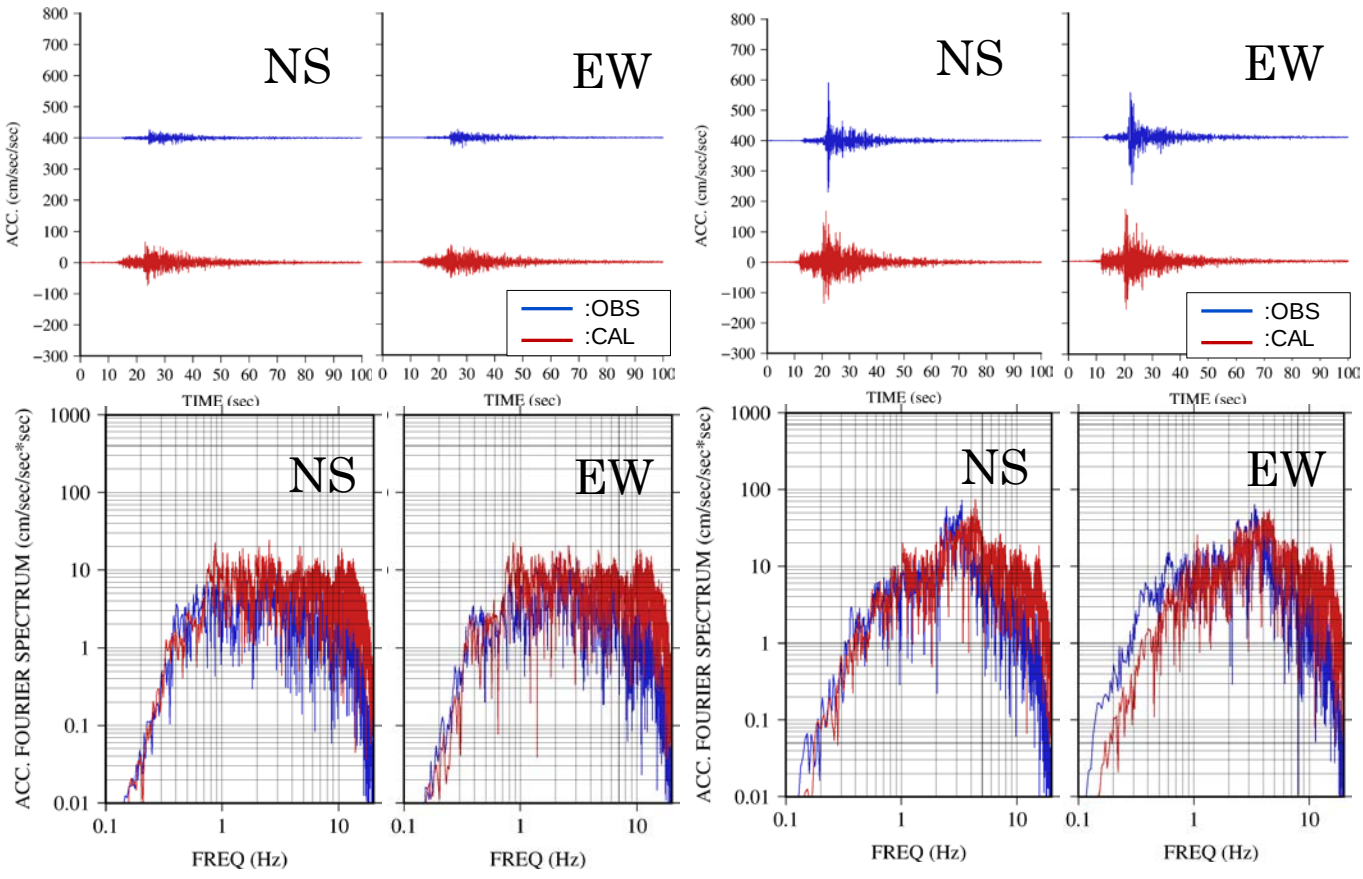

(a) IBR011(Tshukuba) (b) CHB003 (Shirai)

Fig. 3 – Comparison of calculations and observations

Figs. 3(a) and (b) (IBR011 (Tsukuba) and CHB003 (Shirai), respectively) show comparisons of the calculation results and observations (acceleration waveforms and Fourier spectra). The red solid lines denote the calculation results, while the blue solid lines represent the observation records. The left ones in each figure show the NS direction, whereas the right ones show the EW direction. Looking at the seismic waves, one might understand that the shape and amplitude of the waveforms are similar. Moreover, the comparison of the spectra shows the trends of the same frequency characteristics. Therefore, the strong motion simulation based on the PPSM is confirmed to be an effective technique as a predictive problem for the northwestern Chiba Prefecture earthquake in 2005. However, the corner frequency (similar to the stress drop) is higher than the average value commensurate with its seismic-moment M_0 (we set the corner frequency by referring to Nagasaka et al. [15]). The parameters related to source characteristics, such as the concept of stress drop and radiation in a source, need to be considered.

3.2 The mid Niigata prefecture earthquake in 2004

3.2.1 Considering non-linear effects to site factors

The ground motions observed at a particular site (target site) have the source characteristics (source), propagation effects of seismic waves (pass), and site amplification (site). A site amplification, which is also called “site factor” or “empirical site amplification,” is often used as the amplification from the bedrock to the surface.

The empirical site amplification, for example, is estimated from the observation records of the seismic waves using the spectral inversion methods introduced by Iwata and Irikura [16]. Nakano et al. [11] estimated the characteristics of the strong ground motions as the average properties that excluded the non-linear effects. Some of the observed waveforms at a particular site in a large earthquake contain all of the effects, such as the non-linear effects and propagations from the source to the surface at a site. Accordingly, empirical site amplification is defined as the ratio of the Fourier spectra of the observed waveforms divided by the products of a source and a path characteristic, which does not include the non-linear effects considering the non-linear influence. The empirical site amplification characteristics considering the non-linear effects are defined by Eq. (4) as follows:

$$\left|G_{ij}^{N}(f)\right| = O_{ij}^{N}(f) \Big/ \left|S_i(f)\right| \cdot \left|P(f)\right| \tag{4}$$

where $G(f)$ is the empirical site amplification considering the non-linear effects; $O(f)$ is the acceleration Fourier spectrum of the observed waveform at the site, where the non-linear effects are suspected in a large-scale earthquake; $S(f)$ and $P(f)$ are the seismic source and propagation characteristics, respectively, estimated by the spectral inversion method. Suffix “N” indicates that the non-linear effects are included. Subscripts “i” and “j” denote the i-earthquake and j-observation sites, respectively. | | is the absolute value.

3.2.2 Comparison of calculations and observations

Table 2 shows the simulation parameters by the PPSM to the mid Niigata prefecture earthquake in 2004. The seismic moment M_0 is calculated using the F-net.

Table 2 – Simulation parameters of the mid Niigata prefecture earthquake in 2004

Seismic moment M_0 (N・m)	$1.24*10^{19}$
Corner frequency (Hz)	0.11
Radiation coeficient	0.63
FS	2
PRTITN	$1/\sqrt{2}$
Dentisy of seismic bedrock (g/m^3)	3.2
Vs(m/s)	3600
Site amplification	Nakano et al. [11]
Phase characteristics	Observation records (6th Augest, 2004; M_{JMA}4.6)

We assumed a point source as the hypocenter because our objective is to verify the PPSM as a simple method to simulate the strong ground motions of earthquakes that occurred in the past. This earthquake is just an M7 class. The radiation pattern and the P_{RTITN} were set as the average values proposed by Boore and Boatwright [12]. We also use the empirical site amplification estimated by Nakano et al. [11] and the observation records of the earthquake that occurred on August 6, 2004 as the phase characteristics.

Fig. 4 shows the seismic intensity distributions of the simulations and observation records. The calculation results are on the left side of Fig. 4, whereas the observations are on the right side. The stars in the figure denote the earthquake epicenter, while the circles show the observations of the K-NET or KiK-net. The seismic intensity is expressed for colors in the circles followed by the contour scale below the figure. Accordingly, SI in Fig. 4 stands for seismic intensity. The seismic intensities are calculated, using the method proposed by Fujimoto and Midorikawa [17]. The mechanism solution of the earthquake calculated by the F-net is shown in the same figure. The seismic intensity calculated by the PPSM in NIGH11 and NIG023, which are close to the epicenter, is in a good agreement with the observations. Both distributions in the seismic intensity are similar.

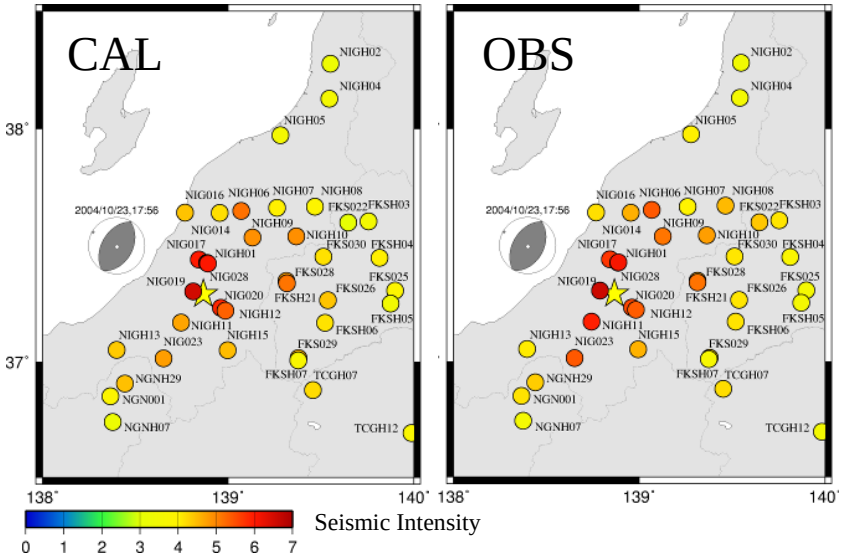

Fig. 4 – Distributions of the seismic intensity (left: calculations, right: observations)

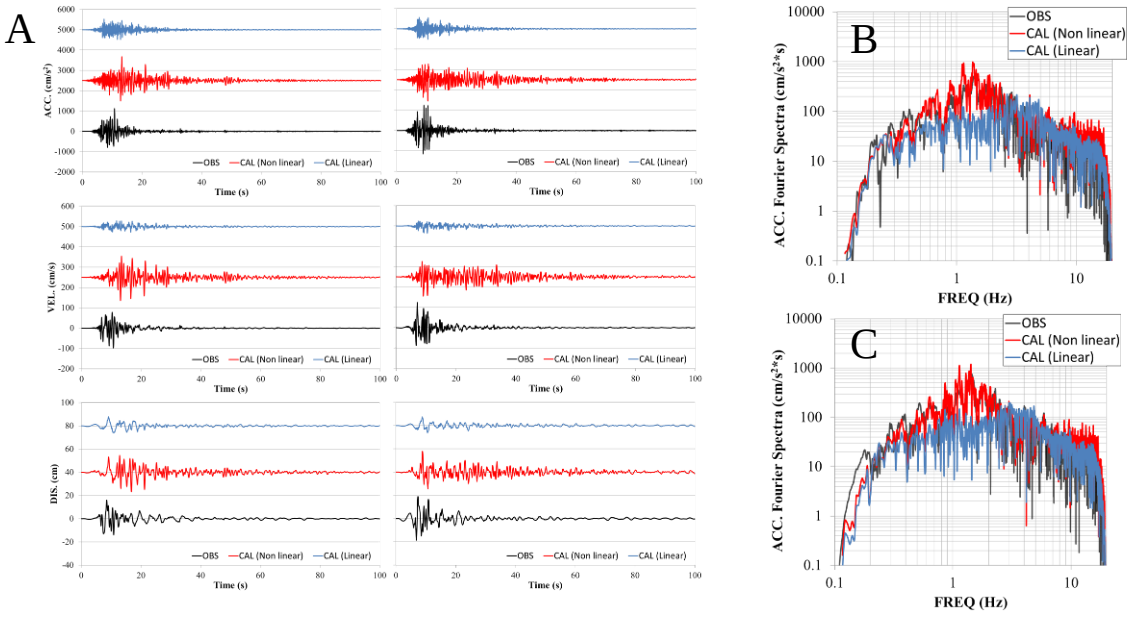

Fig. 5 – Comparison of the calculations and observations for the seismic waves and the Fourier spectra

Fig. 5 shows the comparison of the calculations and observations for the seismic waves and the Fourier spectra. Fig. 5A presents the comparison of the seismic waves at NIG019 (left: NS direction, right: EW direction). Figs. 5B and C show the comparison of the acceleration Fourier spectra (B: NS direction, C: EW direction). The blue line herein represents the calculation results using the linear site amplification. The red line denotes the calculation results using the site amplification, including the non-linear effects estimated by Eq. (4). The black line represents the observations. Upon considering the non-linear influence, as compared to the case that does not consider this, the amplitude of the Fourier spectra is found to be in good agreement with the observed ones. The seismic waves of the calculated acceleration, velocity, and displacement are similar to the observed ones.

3.3 The northern Nagano prefecture earthquake in 2014

Table 3 shows the simulation parameters in the Nagano prefecture Kamishiro fault earthquake. The seismic source herein is assumed as the point source considering the size of the target earthquake. The radiation pattern and P_{RTITN} are the average values. We use the empirical site amplification of linear estimated by Nakano et al. [11]. We also utilize the observation records of aftershocks that occurred on November 23, 2014 (M_{JMA}4.4) as the phase characteristics.

Fig. 6 shows the comparison of the seismic intensity distributions. The left side on Fig. 6 shows the seismic intensity distributions of the observation records (OBS), whereas the right one shows the seismic intensity distributions of the calculation results estimated by the PPSM (CAL). The seismic intensities are calculated following the method used by Fujimoto and Midorikawa [17]. The stars in the figures show the earthquake epicenter, while the circles indicate the observations in the K-NET or KiK-net. SI in Fig. 6 stands for seismic intensity. Both distributions of the seismic intensity are similar. We can reproduce the seismic intensity distributions of observations at the sites away from the source (e.g., NGN014 (Koume)) more than in near sites (e.g., NGNH28 or NGN002).

Table 3 – Simulation parameters for the mid Niigata prefecture earthquake in 2004

Seismic moment M_0 (N・m)	$2.76*10^{18}$
Corner frequency (Hz)	0.17
Radiation coeficient	0.63
FS	2
PRTITN	$1/\sqrt{2}$
Dentisy of seismic bedrock (g/m^3)	3.2
Vs(m/s)	3600
Site amplification	Nakano et al. [11]
Phase characteristics	Observation records (23th November, 2014; M_{JMA}4.4)

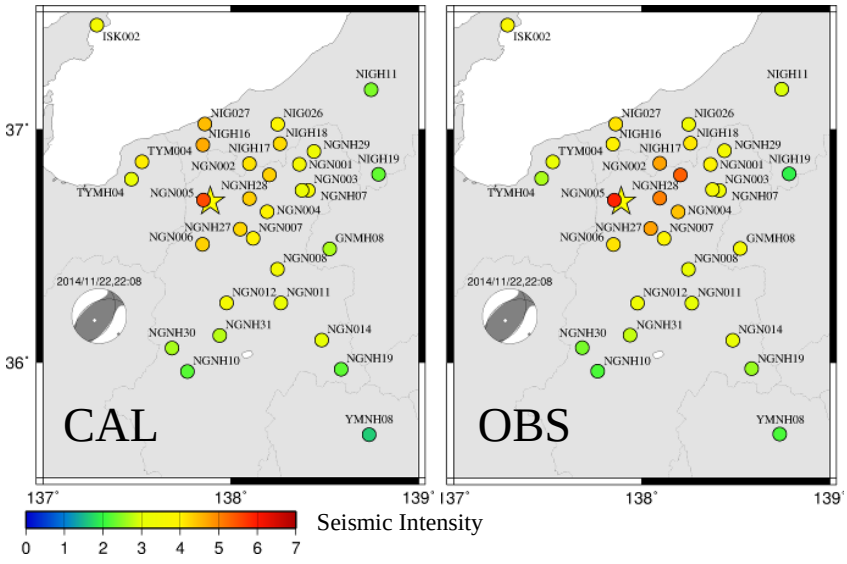

Fig. 6 – Distributions of the seismic intensity (left: calculations, right: observations)

4. Tokachi-oki earthquake in 2003

Tokachi-oki earthquakes occur periodically off the coast of the Hokkaido Tokachi region in Japan. In 2003, the earthquake with M_{JMA}8.0 magnitude occurred off the coast of the Hokkaido Tokachi region. During the earthquake, the Fire and Disaster Management Agency in Japan reported 849 injured and two dead or missing persons. A total of 2064 buildings were damaged by the earthquake [18].

The seismic waveforms of Tokachi-oki earthquake in 2003 have been calculated by researchers [6, 19] performing the inversion method to estimate the fault plane properties. Among them, the fault model with three strong motion generation areas (i.e., SMGA or asperity, in general) proposed by Kamae and Kawabe [6], who used the empirical Green's function method (EGFM) based on the strong motion prediction recipe [20, 21], accurately reproduces the observation records in their paper. Nozu [8] determined the proper placements of the point sources (i.e., sub-events) using the strong ground motion simulations of the Tohoku earthquake in 2011. However, determining the proper placement of point sources on the fault planes of mega earthquakes larger than the M8 class is difficult as the prediction problems. Therefore, we adopt the procedure of the strong motion prediction recipe to determine the placements of the sub-events. We also assume the three point sources on the fault plane proposed by Kamae and Kawabe [6] (Fig. 7).

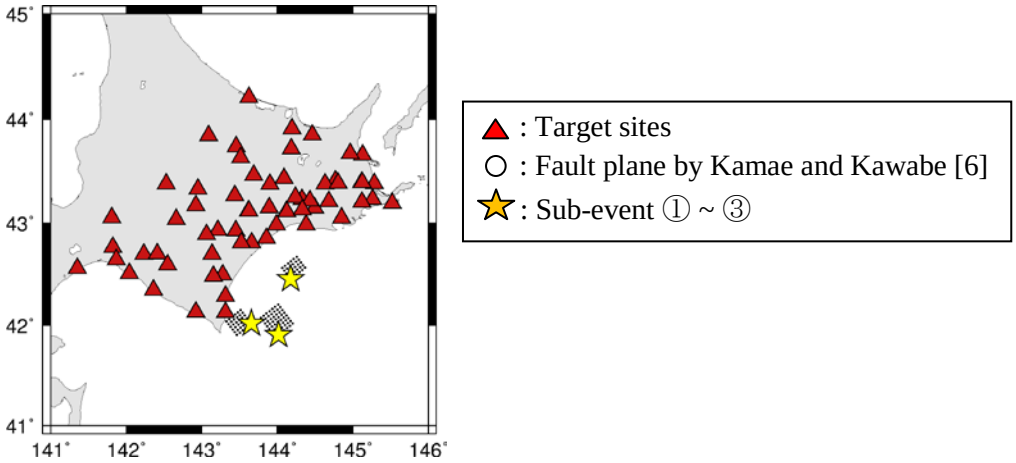

Fig. 7 – Target sites and sub-events are used in this simulation: fault plane proposed by Kamae and Kawabe [6]

The sub-events are shown as star symbols for the PPSM. The fault plane proposed by Kamae and Kawabe [6] is shown as circles. The triangles represent the target points of calculations in the K-NET or KiK-net in Fig. 7. We model the fault plane proposed by Kamae and Kawabe [6] as the only three sub-events (① – ③) on the SMGA. We select two aftershocks of the Tokachi-oki earthquake in 2003 as the phase characteristics of each sub-event. Table 4 shows the simulation parameters for the Tokachi-oki earthquake in 2003. Each of sub-event location corresponds to the SMGA in the fault plane. The corner frequency is estimated to be fitting into the source spectrum assuming the ω^{-2} model using the values of the stress drop estimated by Kamae and Kawabe [6]) in each sub-event.

Table 4 – Simulation parameters for the Tokachi-oki earthquake in 2003

Parameter	Sub-event ①	Sub-event ②	Sub-event ③
Seismic moment M_0 (N・m)	$1.99*10^{20}$	$8.75*10^{19}$	$6.43*10^{19}$
Corner frequency (Hz)	0.01	0.13	0.14
Radiation coeficient	0.63		
FS	2		
PRTITN	$1/\sqrt{2}$		
Dentisy of seismic bedrock (g/m^3)	3.2		
Vs(m/s)	4000		
Site amplification	Nakano et al. [11]		
Phase characteristics	Observation records (26th September, 2003; M_{JMA}5.4)		Observation records (27th September, 2003; M_{JMA}5.2)

Fig. 8 shows the comparison of the seismic intensity distributions of the calculations and the observations. The figure on the right side in Fig. 8 shows the seismic intensity distributions of the observation records (OBS). The figure on the left side in Fig. 8 is the seismic intensity distributions of calculations (CAL). The seismic intensities are estimated by Fujimoto and Midorikawa [17]. The stars show the sub-events on the fault plane of the earthquake. The mechanism solution of the earthquake estimated by the F-net is also shown. The overall trend of the seismic intensity distributions is confirmed to be reproduced by the calculation comparing to the observation. Fig. 9 shows the comparison of PGA and Sa (h=5%) between observations and calculations. We can see that the PGA of calculations are accommodate with observation ones, and, Sa (h=5%) of calculations are good agreement to observation ones at 0.1s. It suggests us that the calculation is going well in short-period range.

Fig. 10 shows the comparison of the waveform calculations and the observations with the seismic waves and the acceleration Fourier spectra at HKD098 (Taiki) and KSRH09 (South-shironuka). Fig. 10 (a) shows the results at HKD098 (Taiki), while Fig. 10 (b) shows those at KSRH09 (South-shironuka). The figures on the left side of Figs. 10 (a) and (b) show the NS direction. The figures on the left side show the EW direction. The seismic waves with acceleration, velocity, and displacement from the top are shown. The acceleration Fourier spectra is shown in the bottom of the figure. The black solid lines show the observation records (OBS), whereas the red solid lines show the calculations (CAL). From the comparison in Fig. 10, the amplitude and shape of the waveforms obtained by the calculation are similar to the observation ones. The characteristics of the Fourier spectra obtained using the calculation are in good agreement with the observation ones as same as seismic waves.

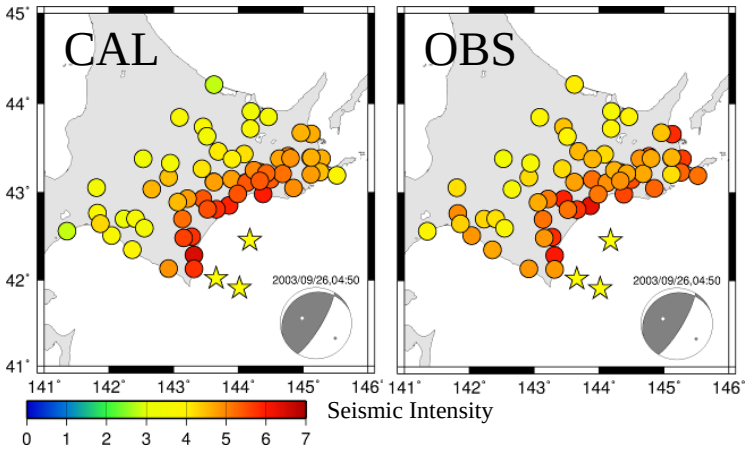

Fig.8 –Distributions of the seismic intensity (left: calculations, right: observations)

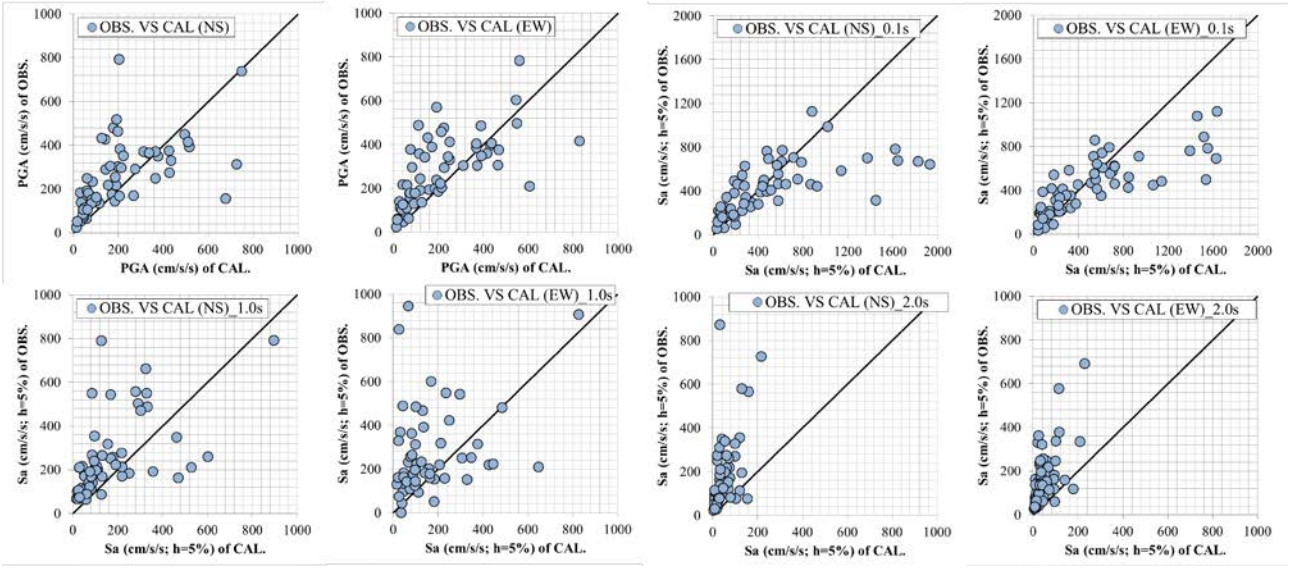

Fig. 9 – Comparison of PGA and Sa (h=5%) between OBS. And CAL.

5. Conclusion

We verified the simulation method based on the PPSM proposed by Nozu (2010) by simulating three crustal earthquakes and a plate-boundary earthquake in Japan using the empirical site amplification estimated by Nakano et al. [11]. The results are different from what Nozu (2010) used, which means that we have confirmed the validity of the PPSM, or, we would be able to pass the verification of this method. However, our study is just one of the samples for verifications and validations of the PPSM under the condition shown here. Therefore, we have to continue developing the strong ground motion prediction methods by verifications and validations to observe records and synthesize them for future mega-earthquakes.

6. Acknowledgment

We used the strong motion records provided by the National Research Institute for Earthquake Science and Disaster Prevention (NIED) in this study. We also used generic mapping tools [22]. This study was partially supported by MEXT/JSPS Grand-in-Aid for Basic Research (A) No. 26242037 (P.I. Hiroshi Kawase). The fault plane model of the Tokachi-oki earthquake in 2003 was provided by Prof. Kamae from Kyoto University. We are grateful for these.

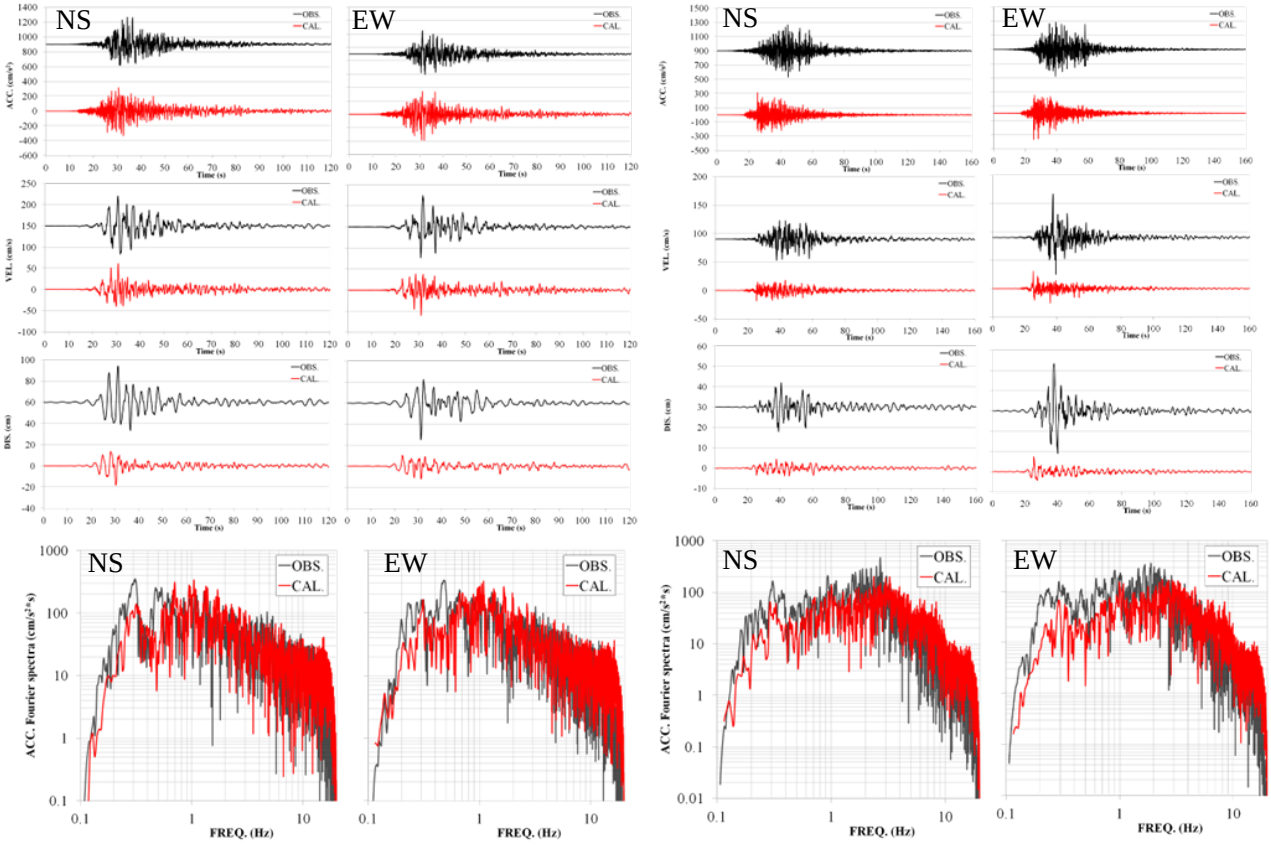

(a) HKD098 (Taiki)

(b) KSRH09 (South-Shiranuka)

Fig. 10 – Comparison of the calculations and observations

7. References

[1] Hartzell S.H. (1978) : Earthquake aftershocks as Green's function, *Geophys. Res. Lett.*

[2] Irikura K. (1986) : Prediction of strong acceleration motion using empirical Green's function, *Proc. 7th Japan Eathquake Symp.*

[3] Irikura, K. (1988) : Estimation of near-field ground motion using empirical Green's Function, *Proc. of 9th World Conf. on Earthq. Eng.*

[4] Irikura, K., Kagawa T., and Sekiguchi H. (1997) : Revision of the expirical Green's function method, English translation of the paper published on B25 of „PROGRAMME and ABSTRACTS", *Seismological Society of Japan* (in Japanese).

[5] Kamae, K. and Irikura K. (1995) : A fault rupture model of the 1995 Hyogoken Nambu earthquake (MJMA = 7.2) estimated by the empirical Green's function method, *J. Natural Disas. Sci.*

[6] Kamae K. and Kawabe H. (2004) : Source model composed of asperities for the 2003 Tokachi-oki, Japan earthquake (M_{JMA} = 8.0) estimated by the empirical Green's function method, *Earth Planets Space.*

[7] Hisada Y. (1994) : An efficient method for computing green's functions for a layered half-space, *Bull. Seism. Soc. Am* (Part 2 published in 1995).

[8] Nozu A. (2012) : A simplified source model to explain strong ground motions from a huge subduction earthquake-simulation of strong ground motions for the 2011 off the Pacific coast of Tohoku earthquake with a pseudo point-source model, *J. Seism. 2.*

[9] Hata, Y. and Nozu A. (2014) : Pseudo point-source models for shallow crustal earthquakes in Japan, *Proc. of the Second European Conference on Earthquake Engineering and Seismology.*

[10] Boore D.M. (1983) : Stochastic simulation of high-frequency ground motions based on seismological models of the radiated spectra, *Bull. Seismol. Soc. Am.*

[11] Nakano K, Matsushima S., and Kawase H. (2015) : Statistical properties of strong ground motions from the generalized spectral inversion of data observed by K-NET, KiK-net, and the JMA Shindokei Network in Japan, *Bull. Seism. Soc. Am.*

[12] Boore D.M. and Boatwright, J. (1984) : Average body-wave radiation coefficients, *Bull. Seismol. Soc. Am.*

[13] Hisada et al. (2012–2014). Benchimark test for the methods of strong ground motion predictions (http://kouzou.cc.kogakuin.ac.jp/benchmark.htm).

[14] Nakano K., Sakai S., Ishikawa A., and Hisada Y. (2015) : Benchmark tests for strong motion simulation in the Tokyo metropolitan area: part 2 prediction method based on pseudo point-source model, *Architectural Institute of Japan.*

[15] Nagasaka Y., Nozu A., and Wakai A. (2016) : Strong ground motion simulation for the 2005 central Chiba prefecture earthquake with pseudo point-source model, *Bull. J. Association for Earthquake Engineering.*

[16] Iwata T., and Irikura K. (1984). Estimation of irregular underground-structure form seismic ground motions, *Bull. Disas. Prev. Res. Inst.*

[17] Fujimoto K. and Midorikawa S. (2010) : Empirical relationship between JMA instrumental seismic intensity and ground motion parameters considering the effect of earthquake magnitude, *Bull. J. Association for Earthquake Engineering.*

[18] Fire and Disaster Management Agency in Japan (2004) : *The reconnaissance report in the 2003 Tokachi-oki earthquake* (in Japanese).

[19] Honda R., Aoi S., Morikawa N., Sekiguchi H., Kunugi T., and Fujiwara H. (2004) : Ground motion and rupture process of the 2003 Tokachi-oki earthquake obtained from strong motion data of K-NET and KiK-net, *Earth Planets Space.*

[20] Irikura K. (1999) : Recipe for estimating strong ground motions from active fault earthquakes, *Proc. International Workshop on Seismotectonics at the Subduction Zone — Toward the Breakthrough in the Next Century*, National Research Institute for Earth Science and Disaster Prevention Science and Technology Agency, Tsukuba, Japan.

[21] Irikura K. (2000) : Recipe for predicting strong ground motion, *US–Japan Cooperative Research for Urban Earthquake Disaster Mitigation Workshop on Prediction of Strong Ground Motions in Urban Regions*, Tokyo Ruby Hotel (Tokyo).

[22] Wessel, P. and Smith W.H.F. (1998) : New, improved version of generic mapping tools released, *Eos Trans.* AGU.